

First-principles study of superconductivity in high-pressure Boron

D. A. Papaconstantopoulos and M. J. Mehl

Center for Computational Materials Science, Naval Research Laboratory, Washington, D.C. 20375-5345

(Dated: July 24, 2013)

We study superconductivity in Boron using first-principles LAPW calculations, the rigid-muffin-tin approximation and the McMillan theory. Our results point to an electron-phonon mechanism producing transition temperatures near 10K at high pressures in agreement with recent measurements.

PACS numbers: 74.70.-b, 71.20.Dg, 71.20.-b

I. INTRODUCTION

In a recent paper Eremets et al.¹ reported experiments where boron transforms from a non-metal at normal pressures to a superconductor at very high pressures above 160 GPa. They presented results that showed an increase of the superconducting temperature, T_c , from 6K at 175 GPa to 11K at 250 GPa.

Previous theoretical studies on the metallization of boron based on first-principles total-energy calculations² predicted that the 12 atom insulating form of boron ($\sqrt{2} \times \sqrt{2} \times 1$ B) at atmospheric pressure transformed to a metallic body-centered tetragonal phase at 210 GPa and subsequently to an fcc structure at 360 GPa.

In this work we performed total energy and band structure calculations for the rhombohedral $\sqrt{2} \times \sqrt{2} \times 1$ B and fcc phases. Our results for the fcc phase were used as an input to the rigid-muffin-tin (RMT) theory of Gaspari and Gyor'ffy³ to determine the value of the Hopfeld parameter and subsequently evaluate the coupling constant and T_c . Our results for the parameter give values comparable to those reported in the past⁴ for metallic hydrogen at very high pressure. Assuming that the fcc phase is the real high pressure structure in the experiments of Eremets et al.¹, this indicates that the simple RMT theory accounts for high-pressure superconductivity in boron.

II. THEORY AND RESULTS

In this work we have applied the RMT theory³ to calculate the Hopfeld parameter given by the expression:

$$H = \frac{E_F}{2N(E_F)} \sum_{\mathbf{l}} 2(l+1) \sin^2(\psi_{\mathbf{l}}) \frac{N_{\mathbf{l}} N_{\mathbf{l}+1}}{N_{\mathbf{l}}^{(1)} N_{\mathbf{l}+1}^{(1)}} \quad (1)$$

where $\psi_{\mathbf{l}}$ is the scattering phase shift at the Fermi energy E_F and angular momentum \mathbf{l} , $N_{\mathbf{l}}^{(1)}$ is the single-scatterer density of states which, as defined in Ref. 3, is an integral involving the radial wave functions. $N(E_F)$ is the total density of states (DOS) at E_F and $N_{\mathbf{l}}$ are the angular momentum components of the DOS inside the muffin-tin spheres. Eq. (1) is exact to $\mathbf{l} = 1$, but for higher values of \mathbf{l} it involves non-spherical corrections. The necessary

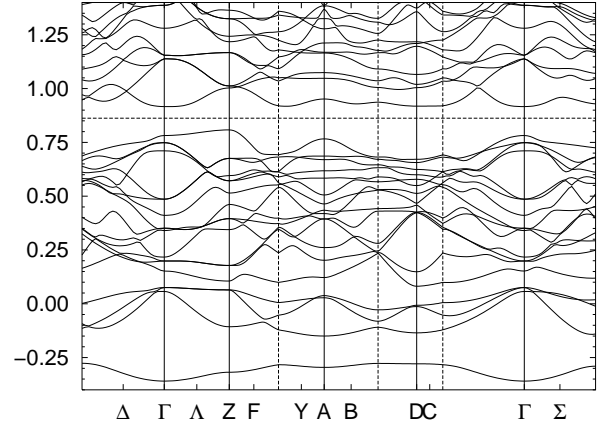


FIG. 1: The electronic band structure of $\sqrt{2} \times \sqrt{2} \times 1$ B, calculated by the LAPW method. The solid vertical lines represent high-symmetry points, while the dashed vertical lines represent zone boundaries. The horizontal line near 0.85 Ry is the Fermi level.

input to Eq. (1) was generated from a set of full-potential Linearized Augmented Plane Wave (LAPW) calculations that we performed for fcc-B using touching muffin-tin spheres, and the tetrahedron method for the DOS.

We also performed an LAPW calculation for $\sqrt{2} \times \sqrt{2} \times 1$ B. This is a rhombohedral structure, space group $R\bar{3}m-D_{3d}^5$ (# 166), with measured lattice parameters⁵ $a = b = c = 9.56$ a.u. and angles $\alpha = \beta = \gamma = 58.06^\circ$. The energy bands of $\sqrt{2} \times \sqrt{2} \times 1$ B are shown in Fig. 1. We obtain a valence bandwidth of 15.9 eV and an energy gap of 1.47 eV separating valence and conduction bands. The angular momentum character of the states can be seen from Fig. 2, which shows the expected dominance of the p-states through the whole spectrum.

For fcc B we calculated an equilibrium lattice parameter $a = 5.37$ a.u. and a bulk modulus of 282 GPa, to be compared with the values of 5.34 a.u. and 269 GPa reported by Maitland et al.² We note that for $a = 4.60$ a.u., which, according to our total energy calculations corresponds to a pressure of 307 GPa, the nearest neighbor B-B distance is 3.25 a.u., which is close to the B-B distance (3.37 a.u.) in the newly discovered superconductor MgB₂. This leads us to believe that superconductivity

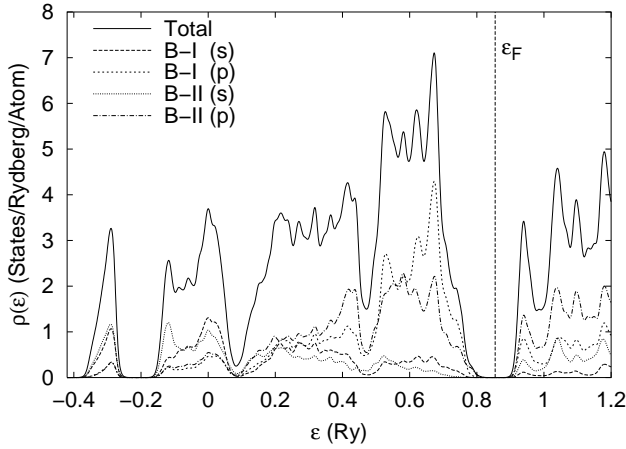


FIG. 2: The electronic density of states of ^{12}B , computed by smearing the eigenvalues of an LAPW calculation using a Fermi temperature of 5 meV. The s and p decomposition is shown for both types of atoms (B-I and B-II) in the ^{12}B structure.

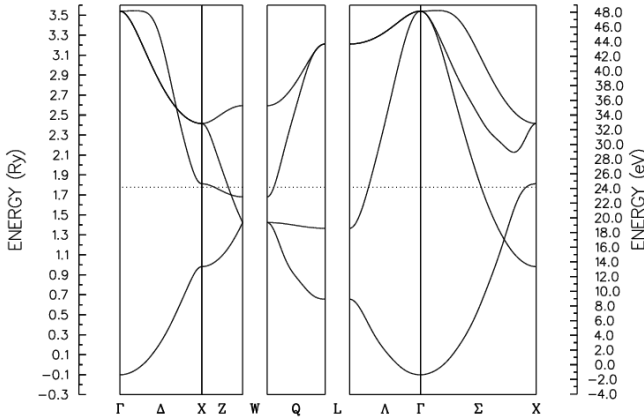


FIG. 3: The electronic band structure of fcc B at the lattice constant 4.60 a.u.

may have the same origin in both materials.

The band structure of fcc B confirms a metallic phase for all lattice parameters, with a rapidly increasing band width going to higher pressures. The occupied band width is 1.43 Ry at equilibrium and 1.88 Ry at $a = 4.60$ a.u. The energy bands for $a = 4.60$ a.u. are shown in Fig. 3. A fairly flat band appears near E_F in the XW direction at all lattice parameters. At X the band has strong s character, becoming p-like at W. This situation is reminiscent of MgB₂ where a similar flat band just above E_F has been identified as the origin of superconductivity in this compound.^{6,7,8,9} This band appears to be responsible for a peak in the DOS at E_F shown in Fig. 4. Also in Fig. 4 we find the s, p, and d distribution of the DOS. In Fig. 4 we confirm that the strongest DOS component is that from p-states. The values of DOS at E_F enter Eq. (1) above for the evaluation of the Hopfeld parameter. The input and results using Eq. (1) at four lattice

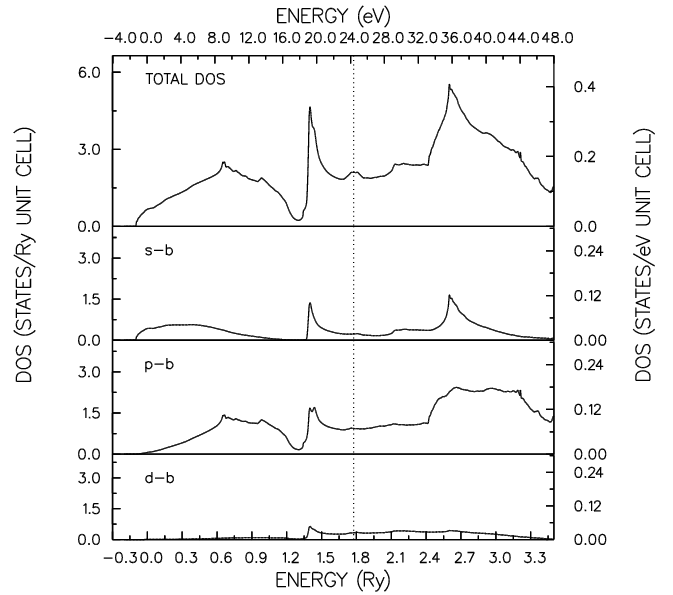


FIG. 4: The electronic density of states of fcc B at the lattice constant 4.60 a.u., as determined by the tetrahedron method.

parameters are listed in Table I.

We note that in Table I the ℓ -components of the DOS are given within the MT spheres (as is the case in Fig. 4), and therefore they do not add up to the value of $N(E_F)$. The p-component, $N_p(E_F)$, is, as expected, dominant and is about 60% of the value of the total inside the MT. The p-d scattering, resulting from the $\ell = 1$ term in Eq. (1), gives by far the largest contribution to the Hopfeld parameter. For the high pressure case ($a = 4.60$ a.u.) $\rho_{pd} = 0.79 \rho_{tot}$. The value of ρ_{tot} is approximately the same as the value of $\rho = 14.13 \text{ eV}/\text{\AA}^2$ previously reported⁴ for metallic hydrogen at a higher pressure of 467 GPa. It is also interesting to note that the boron value of ρ at equilibrium is very close to the value $\rho = 7.627 \text{ eV}/\text{\AA}^2$ for Nb,¹⁰ a typical transition metal superconductor where the d-f scattering is the dominant term in Eq. (1).

To evaluate the critical temperature T_c we have used the McMillan¹¹ approach defining an electron-phonon coupling constant $\lambda = \rho \langle I^2 \rangle$. Here ρ is calculated from Eq. (1) as discussed above. For the average phonon frequency $\langle I \rangle$ we followed Eremets et al.¹ and chose a range of values from 1200K to 1400K. The resulting λ is in the range 0.53 to 0.39 respectively. Continuing we use the McMillan equation:

$$T_c = \frac{\langle I \rangle}{1.45} \exp \left[\frac{1.04(1 + \lambda)}{(1 + 0.62 \lambda)} \right] \quad (2)$$

We solve Eq. (2) for λ values of the Coulomb pseudopotential $\mu = 0.09$ to 0.13, and in the above range of $\langle I \rangle$ and ρ values. The corresponding values of T_c are shown in Fig. 5. Within the uncertainty of the values of the frequency $\langle I \rangle$, and near the value $\langle I \rangle = 1250\text{K}$ our model

TABLE I: Radius of the mu n-tin sphere R_s , Fermi level E_F , Total DOS at E_F , angular components of the DOS N_s , free-scatterer DOS $N_s^{(1)}$, scattering phase shifts δ_s , and δ_s components of the Hop eld parameter μ^* and the total value of μ^* . The three columns are headed by the lattice parameters and the corresponding pressures.

| a (a.u.) | 4:60 | 5:00 | 5:37 | 6:00 |
|-----------------------------------|--------|--------|-------|-------|
| P (GPa) | 307 | 89 | 0 | -50 |
| R_s (a.u.) | 1:626 | 1:768 | 1:898 | 2:121 |
| E_F (Ry) | 1:776 | 1:408 | 1:139 | 0:784 |
| $N(E_F)$ (states/Ry/spin) | 1:050 | 1:328 | 1:475 | 1:514 |
| $N_s(E_F)$ (states/Ry/spin) | 0:114 | 0:172 | 0:233 | 0:276 |
| $N_p(E_F)$ (states/Ry/spin) | 0:469 | 0:568 | 0:637 | 0:769 |
| $N_d(E_F)$ (states/Ry/spin) | 0:164 | 0:193 | 0:195 | 0:155 |
| $N_s^{(1)}$ (states/Ry/spin) | 0:187 | 0:231 | 0:270 | 0:324 |
| $N_p^{(1)}$ (states/Ry/spin) | 0:818 | 1:058 | 1:334 | 1:991 |
| $N_d^{(1)}$ (states/Ry/spin) | 0:010 | 0:105 | 0:106 | 0:099 |
| δ_s | 0:109 | 0:099 | 0:298 | 0:658 |
| δ_p | 0:682 | 0:761 | 0:835 | 0:962 |
| δ_d | 0:031 | 0:029 | 0:027 | 0:021 |
| μ_{sp} (eV /A ²) | 2:945 | 1:576 | 0:820 | 0:150 |
| μ_{pd} (eV /A ²) | 11:555 | 9:172 | 6:960 | 4:048 |
| μ_{df} (eV /A ²) | 0:089 | 0:063 | 0:044 | 0:022 |
| μ_{tot} (eV /A ²) | 14:588 | 10:811 | 7:824 | 4:220 |

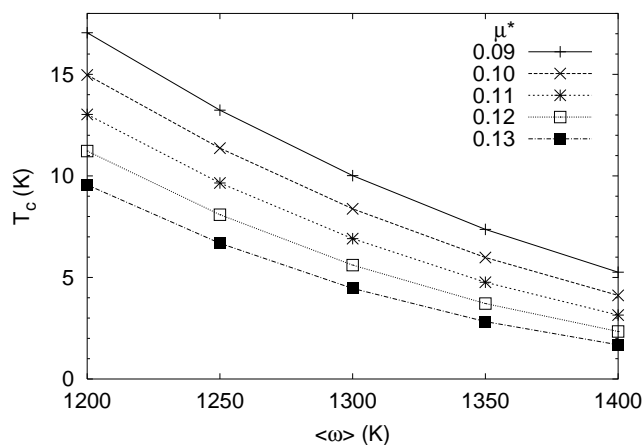


FIG. 5: The superconducting transition temperature T_c of fcc Boron, as determined by the McMillan equation (2), as a function of the RMS phonon frequency $\langle\omega\rangle$ at various values of μ^* .

predicts T_c values in the range of the experiment which

validates the assertion of an electron-phonon mechanism.

Finally, we want to comment on the pressure dependence of T_c . Our calculations show that the parameter μ^* goes from the value 7.82 eV /A² at the equilibrium fcc volume to the value of 14.59 eV /A² at a pressure of 307 GPa. It is important to note that $N(E_F)$ follows the opposite trend, i.e., it reduces with increasing pressure. Assuming that the variation of $\langle\omega\rangle$ with pressure is not as strong as the variation of μ^* we propose that the rapid increase of μ^* is responsible for the observed increase of T_c with pressure.

In summary, we find that LAPW calculations, the RM T theory, and a McMillan analysis for T_c give a good description of superconductivity in boron at high pressures.

Acknowledgments

This work was supported by the U.S. Office of Naval Research.

Electronic address: papaconstantopoulos@dave.nrl.navy.mil

^y Electronic address: mehl@dave.nrl.navy.mil

¹ M. I. Eremin, V. V. Stuzhkin, H. Mao, and R. J. Hemley, Science 293, 272 (2001).

² C. M. Ailhiet, J. B. Grant, and A. K. McMillan, Phys. Rev. B 42, 9033 (1990).

³ G. D. Gasparyan and B. L. Gyorffy, Phys. Rev. Lett. 28, 801 (1972).

⁴ D. A. Papaconstantopoulos and B. M. Klein, Ferroelectrics

16, 307 (1977).

⁵ P. Villars and L. Calvert, eds., Pearson's Handbook of Crystallographic Data for Intermetallic Phases (ASM International, Materials Park, Ohio, 1991), 2nd ed.

⁶ J. M. An and W. E. Pickett, Phys. Rev. Lett. 86, 4366 (2001).

⁷ J. Kortus, I. I. Mazin, K. D. Belashchenko, V. P. Antropov, and L. L. Boyer, Phys. Rev. Lett. 86, 4656 (2001).

⁸ M. J. Mehl, D. A. Papaconstantopoulos, and D. J. Singh,

- Phys. Rev. B 64, 140509(R) (2001).
- ⁹ Y. Kong, O. V. Dolgov, O. Jepsen, and O. K. Andersen, Phys. Rev. B 64, 020501 (2001).
- ¹⁰ D. A. Papaconstantopoulos, L. L. Boyer, B. M. Klein, A. R. Williams, V. L. Moruzzi, and J. F. Janak, Phys. Rev. B 15, 4221 (1977).
- ¹¹ W. L. Moruzzi, Phys. Rev. 167, 331 (1968).